JGR Space Physics

Key Points:
- The solar wind energy dissipated in the Earth's upper atmosphere is higher than it would be if the Earth were not magnetized

Correspondence to:
R. Maggiolo,
maggiolo@aeronomie.be

The Earth's Magnetic Field Enhances Solar Energy Deposition in the Upper Atmosphere

R. Maggiolo[1] , **L. Maes[2]** , **G. Cessateur[1]** , **F. Darrouzet[1]** , **J. De Keyser[1,3]** , and **H. Gunell[4]**

[1]Royal Belgian Institute for Space Aeronomy (BIRA-IASB), Brussels, Belgium, [2]Max Planck Institute for Solar System Research, Göttingen, Germany, [3]Center for Mathematical Plasma Astrophysics, KULeuven, Heverlee, Belgium, [4]Department of Physics, Umeå University, Umeå, Sweden

Abstract The presence of a large-scale planetary magnetic field is thought to be a protective factor for atmospheres, preventing them from being blown off by the solar wind. We focus on one key aspect of atmospheric escape: how does a planetary magnetic fields affect the energy transfer from the Sun to the atmosphere? We estimate the solar wind energy currently dissipated in the Earth's atmosphere using empirical formulas derived from observations. We show that it is significantly higher than the energy dissipated in the atmosphere of a hypothetical unmagnetized Earth. Consequently, we conclude that the Earth's magnetic field enhances the solar energy dissipation in the Earth's atmosphere and that, contrary to the old paradigm, an intrinsic magnetic field does not necessarily reduces atmospheric loss.

1. Introduction

The Sun is the dominant energy source for ionizing atmospheric material and energizing a fraction of it to energies above the gravitational binding energy. Solar energy is transferred to the atmosphere mainly through solar ultraviolet and extreme ultra violet (UV/EUV) radiation and via the solar wind, a continuous flow of plasma emitted by the Sun and embedded in the Interplanetary Magnetic Field (IMF). In the following, we do not consider the energy deposition by solar photons in the planetary atmosphere as it is independent of the planetary magnetic environment. Solar wind energy is mainly dissipated in the upper atmosphere. It includes energy dissipation in the ionosphere, that is, the transfer of energy to the ionized component of the upper atmosphere, and in the thermosphere, that is, the transfer of energy to the neutral component of the upper atmosphere.

The coupling between the solar wind and the ionosphere is mediated by the planetary magnetosphere, both for the magnetospheres of magnetized planets like Earth and for the induced magnetospheres of unmagnetized planets like Venus and Mars. Extensive measurements of ion outflow from Venus, Earth and Mars have shown that the escape rates are similar from all three planets, if not higher for Earth than for the other two. This suggest that an intrinsic magnetic field is not required to prevent ion escape, contrary to the old paradigm (Gunell et al., 2018; Maggiolo & Gunell, 2021; Ramstad & Barabash, 2021).

Ion escape involves many steps (Gronoff et al., 2020), from the ionisation of neutral atmospheric material to the acceleration and transport of planetary ions into interplanetary space. Each of these steps, like the solar wind energy transfer to the upper atmosphere, the ion supply in the ionosphere or the efficiency of the acceleration processes, can act as a bottleneck and limit the amount of ionized material that can be removed from the atmosphere.

The energy carried by the solar wind and IMF is the sum of the kinetic energy of the bulk flow of the particles, the enthalpy of the solar wind plasma and the electromagnetic energy. At Earth, the solar wind energy flux is dominated by the kinetic energy of the wind which is roughly two orders of magnitude larger than the electromagnetic energy (Lockwood, 2019) while the contribution of enthalpy is negligible (Le Chat et al., 2012).

The Earth's magnetosphere acts as a shield that diverts most of the solar wind flow so that a small fraction of the incoming solar wind energy enters the magnetosphere (Wing et al., 2014). Once in the magnetosphere, the solar wind energy can either be dissipated in the magnetosphere, in the ring current region and in the magnetospheric tail, or be dissipated in the upper atmosphere. The proportion of energy dissipated in the upper atmosphere represents approximately 1%–10% percent of the solar wind energy entering the magnetosphere (Knipp et al., 1998; Li et al., 2012; Østgaard, Germany, et al., 2002; Tenfjord & Østgaard, 2013). However, the Earth's magnetosphere is much larger than the Earth itself. The solar wind compresses its sunward side to a typical distance of 10 Earth

radii while its night-side is much more extended, possibly up to 1,000 Earth radii. At the level of the Earth, the cross section of the magnetosphere with the solar wind is more than 200 times larger than the cross section of the Earth with the solar wind. The Earth intrinsic magnetic field thus generates a large scale magnetosphere which has two opposite effects. On the one hand, it efficiently diverts the solar wind flow from the upper atmosphere and only a small fraction of the solar wind energy flux it intercepts eventually ends up being dissipated in the upper atmosphere. On the other hand, a large scale magnetosphere dramatically increases the area of interaction between the solar wind and the Earth and thus the amount of solar wind energy that may potentially be funneled into the upper atmosphere.

In the upper atmosphere, solar wind energy dissipates through various mechanisms. The solar wind plasma, as it flows past the Earth's magnetosphere, generates a large scale electric field that drives the plasma circulation in the high-latitude ionosphere. Ionospheric Joule heating refers to the energy dissipated by collisions between plasma and neutrals due to their resulting relative motion (Vasyliūnas & Song, 2005). This is the dominant channel for solar wind energy dissipation in the upper atmosphere. Solar wind energy is also dissipated through particle precipitation. Particle precipitation mostly occurs at high latitude. In the dayside high latitude upper atmosphere, particle precipitation is dominated by the precipitation of solar wind material in the cusp region. In the nightside high latitude upper atmosphere, the precipitating particles consist of solar wind and ionospheric plasma that has been accelerated in the magnetosphere. Precipitating particles transfer their energy to the upper atmosphere through collisions. The solar wind interaction with the Earth's magnetic field generates a variety of waves (Thorne et al., 2021). These carry electromagnetic energy that can be dissipated in the upper atmosphere. In particular Ultra Low Frequency Waves (ULF which in the context of magnetospheric physics refers to electromagnetic waves with frequencies below ∼5 Hz) can contribute significantly to electromagnetic energy flow from the magnetosphere to the high-latitude ionosphere during geomagnetically active periods. Among the ULF waves, Alfven waves transfer energy along the background magnetic field direction and likely represent the dominant wave mode (Hartinger et al., 2015). ULF wave energy is dissipated in the upper atmosphere through collisions between ions and neutrals due to their relative motion induced by the waves (similar to ionospheric Joule heating for quasi stationary electromagnetic fields).

Joule heating, particle precipitation and waves are the three main pathways for energy dissipation in the upper atmosphere. Other processes may contribute to a lesser extent.

A large scale magnetosphere like the Earth's can store solar wind energy and release it abruptly in the upper atmosphere during storm or substorm time periods. This sudden release of energy results in variations of the magnetic field that are measured by ground stations from which geomagnetic activity indices are derived. The time response of the magnetospheric activity to the solar wind driver varies from a few minutes to tens of hours (Maggiolo et al., 2017). There is thus no immediate correspondence between the solar wind incoming energy level and the energy dissipation in the upper atmosphere as they are mediated by the magnetosphere. Empirical formulas derived from observation therefore describe the energy deposition in the upper atmosphere as a function of geomagnetic indices rather than solar wind parameters.

This study focuses on a particular aspect of the chain of processes leading to ion loss: the energy transfer from the Sun to the upper atmosphere. The goal is to assess the protective effect of planetary magnetic fields on the upper atmosphere, and more specifically to assess if the Earth's magnetosphere enhances the solar energy dissipation in the Earth's upper atmosphere as suggested by Maggiolo and Gunell (2021).

To do so, we compare the energy dissipated by the solar wind in the Earth's upper atmosphere to the maximum energy that would be intercepted by the induced magnetosphere of a hypothetical unmagnetized Earth, which corresponds to the maximal solar wind energy that could be dissipated in the upper atmosphere of the Earth if it were unmagnetized.

2. Comparing the Incident Solar Wind Energy Input With the Energy Dissipated in the Earth's Ionosphere

2.1. Data

The solar wind data and the geomagnetic indices for the time period considered in this study (from 1 January 1963 to 31 December 2020) are extracted from the OMNI data set through the OMNIWeb (http://omniweb.gsfc.nasa.gov).

We use 1 hr resolution solar wind parameters propagated to the nominal magnetospheric bow shock. The details of the method used to compute 1 hr averaged data and to propagate solar wind data to the nose of the bow shock can be found on the OMNIWeb website. Solar wind data are relatively accurate. The solar wind density, velocity, temperature, composition, and the IMF are obtained directly from in-situ measurement and the solar wind incoming energy is directly derived from those observations. The OMNI database is built from measurements made in the solar wind, in particular by the ACE spacecraft located at the Lagrange L1 point. The propagation from the location where the spacecraft makes the measurement to the Earth's magnetosphere may not always be accurate. However, no systematic error on the propagation of the solar wind is expected and thus it may not impact the long term averages on which our conclusions are based. The rate of energy dissipation in the Earth's upper atmosphere is derived from observations. Empirical formulas relating the energy dissipation in the upper atmosphere to geomagnetic indices are obtained from the literature as described below. The actual energy dissipation level for one specific event or time interval may substantially differ from this trend, in particular for extreme events which are less constrained by observations due to their rarity. However, such periods represent a tiny fraction of the data set and do not significantly impact the long term averages.

2.2. Incident Solar Wind Energy

In this section we compute the solar wind energy flux at 1 astronomical unit. It will be used to estimate the solar wind power that would be intercepted by the induced magnetosphere of a hypothetical unmagnetized Earth. The solar wind kinetic energy is mostly carried by the ions, as the bulk velocity of ions and electrons are the same in the solar wind. Here we consider the contribution of the two dominant solar wind ions species, H^+ and He^{++}, which on average represent respectively 95% and 4% of the solar wind ions. Heavier ions are not considered as they represent a small fraction ($\sim$1% all together) (Schwenn, 1990). The solar wind kinetic energy flux density is thus given by:

$$\phi_{Ek} = \frac{1}{2}\left(m_H n_H + m_{He} n_{He}\right) V_{SW}^3 \tag{1}$$

where m_H and m_{He} are the H^+ and He^{++} atomic mass, n_H and n_{He} the H^+, and He^{++} number density and V_{SW} the solar wind velocity.

The solar wind electromagnetic energy flux density is given by the Poynting flux (e.g., Lockwood, 2019):

$$\phi_{EM} = \frac{V_{SW} B^2}{\mu_0}\cos^2\theta \tag{2}$$

where B is the IMF magnitude and θ the angle between the solar wind velocity and magnetic field.

The solar wind interacts with planetary magnetospheres and thus the total amount of solar wind energy that can potentially be diverted toward their upper atmosphere is proportional to the cross section of the magnetosphere with the solar wind. Here we consider a hypothetical unmagnetized Earth in order to estimate the solar wind energy that would be intercepted by its induced magnetosphere. This will be considered as the maximal amount of solar wind energy that could be dissipated in the upper atmosphere of a fictitious unmagnetized Earth for current solar wind conditions. We consider that the cross section of the induced magnetosphere of a hypothetical unmagnetized Earth corresponds to the cross section of its induced magnetosphere at the terminator as delimited by the Induced Magnetosphere Boundary (IMB). The average radial distance of the IMB of a fictitious unmagnetized Earth is estimated to 1.2 R_E by considering the pressure balance between the exosphere and the solar wind and using a Chamberlain exosphere as done by Gunell et al. (2018). For comparison, the average radial distance of the IMB of Mars at the terminator is ~1.5 Martian radii according to observations from Phobos 2 and Mars Global Surveyor (Trotignon et al., 2006), Mars Express (Ramstad, Barabash, Futaana, & Holmström, 2017) and Maven (Matsunaga et al., 2017). The outer boundary of the Venusian induced magnetosphere is located closer to the planet, at radial distances comprised between 1.1 and 1.2 Venus radii according to Venus Express observations (Zhang et al., 2008).

Figure 1 displays the incoming solar wind power intercepted by the induced magnetosphere of a hypothetical unmagnetized Earth. It includes the contribution of the solar wind kinetic energy and Poynting flux as described in Equations 1 and 2, the other components of the solar wind energy flux being negligible. On average, the solar
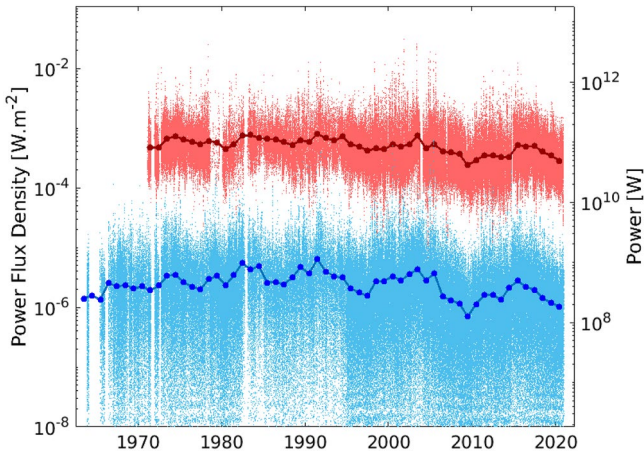
Figure 1. Solar wind energy input at 1 astronomical unit. The left vertical scale represent the solar wind power flux at Earth. The right vertical axis represents the total power intercepted by the induced magnetosphere of a hypothetical unmagnetized Earth. The radius of this induced magnetosphere is fixed to 1.2 Earth radii at the terminator. The red scattered points correspond to the 1 hr averaged solar wind kinetic energy while the blue scattered points represent 1 hr averaged the solar wind Poynting flux. The red and blue solid lines show the yearly average of the solar wind kinetic energy and Poynting flux.

wind kinetic energy flux is approximately two orders of magnitude higher than the Poynting flux. The total power intercepted by the magnetosphere of a hypothetical unmagnetized Earth with a radius of 1.2 R_E is displayed on the right vertical axis.

2.3. Energy Dissipated in the Upper Atmosphere

In this section we estimate the solar wind energy actually dissipated in the Earth's upper atmosphere for the actual (magnetized) Earth, using observations and empirical formulas available in the literature.

The main energy dissipation pathway in the upper atmosphere is Joule heating. Joule heating has been estimated from measurements, large statistical studies, data assimilation methods and simulations (Tenfjord & Østgaard, 2013). The various estimates of the linear relation between the Auroral Electrojet (AE) index and Joule heating based on observations are discussed in details in Østgaard, Germany, et al. (2002). Experimental estimates vary by approximately a factor of 2 (Østgaard, Germany, et al., 2002; Tenfjord & Østgaard, 2013).

A review of several studies based on observations where Joule heating is parametrized as a linear function of the AE index indicates that Joule heating at the solstice is best approximated by the following function (Østgaard, Germany, et al., 2002):

$$U_J[GW] = 0.54AE + 1.8 \tag{3}$$

Joule heating in the Northern Hemisphere as a function of the Polar Cap (PC) index has been estimated using the Assimilative Mapping of Ionospheric Electrodynamics (AMIE) procedure (Chun et al., 1999). The authors proposed the following quadratic functional forms categorized by season:

$$U_J[GW] = 14.39PC^2 + 23.7PC + 11.5 \, (summer)$$
$$U_J[GW] = 4.14PC^2 + 23PC + 8.9 \, (equinox) \tag{4}$$
$$U_J[GW] = 4.84PC^2 + 16.9PC + 5.6 \, (winter)$$

These formulas tend to underestimate Joule heating during strong geomagnetic storms (Chun et al., 1999). This issue has been addressed by adding a dependence on the Disturbance Storm Time (Dst) index (Knipp et al., 2005) with the following functional forms categorized by seasons describing Joule heating as a function of the PC and Dst index:

$$U_J[GW] = 29.27PC + 8.18PC^2 - 0.04Dst + 0.0126Dst^2 \, (summer)$$
$$U_J[GW] = 29.14PC + 2.54PC^2 + 0.21Dst + 0.0023Dst^2 \, (equinox) \tag{5}$$
$$U_J[GW] = 13.36PC + 5.08PC^2 + 0.47Dst + 0.0011Dst^2 \, (winter)$$

Figure 2 shows the 1 hr averaged estimates of the power dissipated via Joule heating given by the functional forms (3–5) from 1963 to 2020. Superposed to it are the corresponding yearly averages. The functional forms (4) and (5) can become negative during periods of very low geomagnetic activity (i.e., for low values of the PC and Dst indices). In that case we set the value to zero as a negative value for the power dissipated by Joule heating is unrealistic. This corresponds to a limited fraction of the data (respectively 3.6% for the functional form (4) and 15.7% for the functional form (5)). Data gaps corresponds to time periods when at least one of the parameters used to determine the energy dissipation was not available. We assume that the dissipated power in the Southern and Northern hemispheres behave similarly to estimate the total dissipated power from the hemispheric values from Equations (4) and (5). For each hemisphere we consider the seasonal variations (summer in the Northern
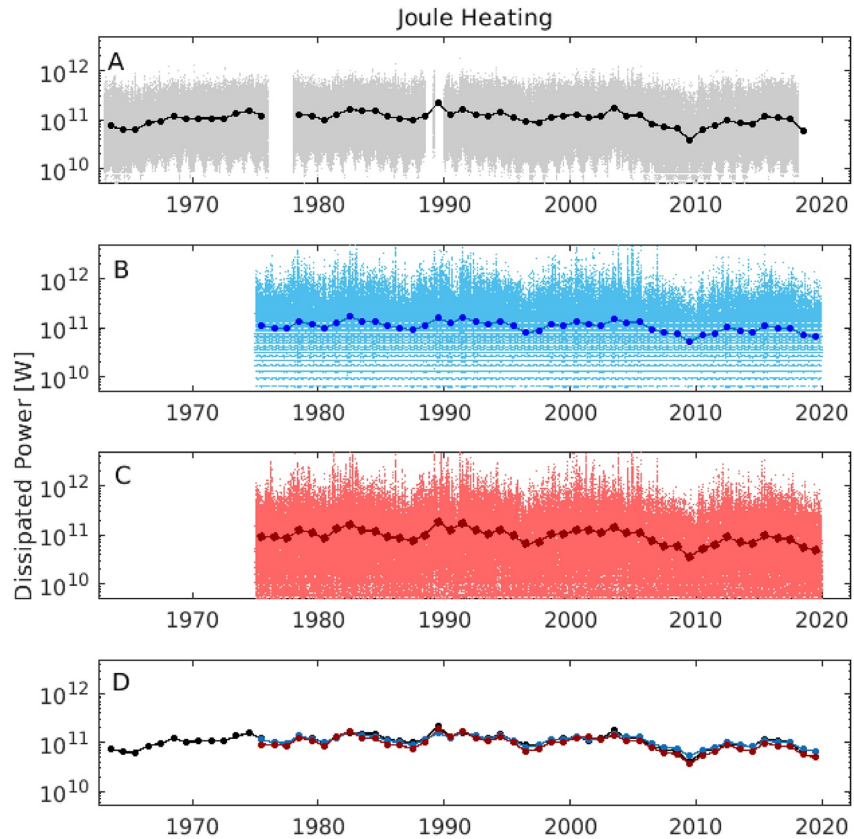
Figure 2. Energy dissipation in the Earth's ionosphere via Joule heating. Panel (a) estimate from the empirical formula from Østgaard, Germany, et al. (2002). Panel (b) estimate from the empirical formula from Chun et al. (1999). Panel (c) estimate from the empirical formula from Knipp et al. (2005). The scattered points represent the 1 hr averaged energy dissipation while the solid lines correspond to the yearly averages. Panel D compares the yearly average of the power dissipated via Joule heating from the three methods using the same colors as in panels (a, b, and c) The yearly averaged dissipated power in 1989 may not be accurate as the AE index is only available for the month of March.

hemisphere and winter in the Southern hemisphere from April 21 to August 20, winter in the Northern hemisphere and summer in the Southern hemisphere from October 21 to February 20 and equinox in both hemispheres from 21 February to 20 April and from 21 August to 20 October). Despite some differences in the estimated 1 hr averaged dissipated power, there is a fairly good agreement between the yearly averaged dissipated power as estimated with these three different functional forms (Figure 2).

In addition to Joule heating, particle precipitation is the second contributor to solar wind energy dissipation in the upper ionosphere. The energy dissipation caused by electron precipitation (between 0.1 and 100 keV) and its relation to the AL index has been derived from UV and X-ray emissions in the Northern Hemisphere during substorm periods (Østgaard, Vondrak, et al., 2002). This relation has been later updated resulting in the following functional form (Tenfjord & Østgaard, 2013):

$$U_e[GW] = 4.3|AL|^{\frac{1}{2}} - 9 \tag{6}$$

This functional form has been determined by deriving the electron energy deposition during seven substorms. It is thus by construction better suited to describe the electron energy deposition during geomagnetically active periods. For periods of low geomagnetic activity (when $|AL| < \sqrt{9/4.3}$) it results in an unrealistic negative value for the energy dissipated in the ionosphere by precipitating electrons.

The AMIE data assimilation method has been used to determine functional forms describing the energy flux of precipitating electrons as a function of the PC index and categorized by seasons (Chun et al., 2002):

$$U_e[GW] = 6.3 \, PC + 21.9 \, (summer)$$
$$U_e[GW] = 9.29 \, PC + 22.6 \, (equinox) \tag{7}$$
$$U_e[GW] = 12.5 \, PC + 31.7 \, (winter)$$

The energy flux of precipitating ions and electrons in the upper atmosphere has been extensively measured by the SSJ/4 instrumental package onboard the DMSP satellites. A statistical analysis of DMSP data (Newell et al., 2009) provided average values of the precipitating electron and ion energy flux for low and high solar wind driving as defined by the solar wind-magnetosphere coupling function proposed by Newell et al. (2007). The energy flux of precipitating ions corresponds to 2.3 GW for low solar wind driving and 4.9 GW for high solar wind driving. For precipitating electrons the energy is estimated to 8.5 GW for low solar wind driving and 30.8 GW for high solar wind driving. Low solar wind driving corresponds to periods when the solar wind-magnetosphere coupling function is lower than 25% of its average value while high solar wind driving is corresponds to periods when it is higher than 50% of its average value (Newell et al., 2009). For intermediate solar wind driving conditions, we consider the average value (obtained for all conditions) of the energy dissipation level (3.4 GW for ions and 17.4 GW for electrons). The energy flux of precipitating ions and electrons for each type of solar wind driving conditions and separated for four auroral precipitation types can be found in Table 1 in Newell et al. (2009).

Figure 3 shows the 1 hr averaged power dissipated via particle precipitation from 1963 to 2020 given by the functional forms (6) and (7) and by the estimates derived from DMSP observations (Newell et al., 2009). Superposed to it are the corresponding yearly averages. These functional forms can become negative during periods of very low geomagnetic activity (i.e., for low values of the AL and PC indices). In that case we set the value to zero as a negative value for the energy dissipation by particle precipitation is unrealistic. This corresponds to a very low fraction of the data (respectively 3.2% for the functional form (6) and 0.16% for the functional form (7)). Data gaps corresponds to time periods when at least one of the parameters used to determine the energy dissipation was not available. We assume that the dissipated power in the Southern and Northern hemispheres behave similarly to estimate the total dissipated power from the hemispheric values from Equation (7). For each hemisphere we consider the seasonal variations (defined the same way as for Joule heating). There is some discrepancy between those three estimates of the power dissipated by precipitating particles (Figure 3). The estimate from the functional form (7) is approximately two times higher than the estimate from the functional form (6) and from DMSP observations. Only the later one consider the energy dissipation related to both precipitating ions and electrons (Newell et al., 2009) while the two functional forms (6) and (7) only consider the contribution of precipitating electrons (Chun et al., 2002; Tenfjord & Østgaard, 2013). However, the contribution of ions to the energy deposition is relatively limited, representing on average 16% of the total energy deposited by precipitating particles (Newell et al., 2009).

ULF waves also contribute to the energy dissipation in the Earth's upper atmosphere. Among them, Alfvén waves constitute the main wave mode that contributes to dissipate energy in the upper atmosphere. The contribution of ULF waves to the total energy dissipation in the upper atmosphere is estimated to a few percent for low to moderately active periods but for intense geomagnetic storm it can contribute to up to ∼30% of the dissipated energy (Rae et al., 2007). The energy carried by Alfvén waves flowing in and out of the Auroral Acceleration Region (AAR) has been quantified by using observations from the FAST and Polar satellites. The following functional forms describing the dependence of the inflowing and outflowing energy of Alfvén waves as observed above the AAR have been built according to those observations (Keiling et al., 2019):

$$AW_{in}[GW] = 0.009 \cdot AE[nT] + 0.070[GW]$$
$$AW_{out}[GW] = 0.003 \cdot AE[nT] - 0.138[GW] \tag{8}$$

The difference between the inflowing and outflowing Alfen wave energy corresponds to the energy that has been lost by Alfvén waves in the AAR and in the upper atmosphere. ∼56% of the incoming Alfven wave power in the auroral zone is transferred to precipitating electrons in the AAR (Keiling et al., 2019). The Alfven wave energy is thus transferred to precipitating electrons above the upper atmosphere and thus is already accounted for when considering the energy flux of precipitating electrons. ∼11% (lower limit) of the incoming Alfven wave power is
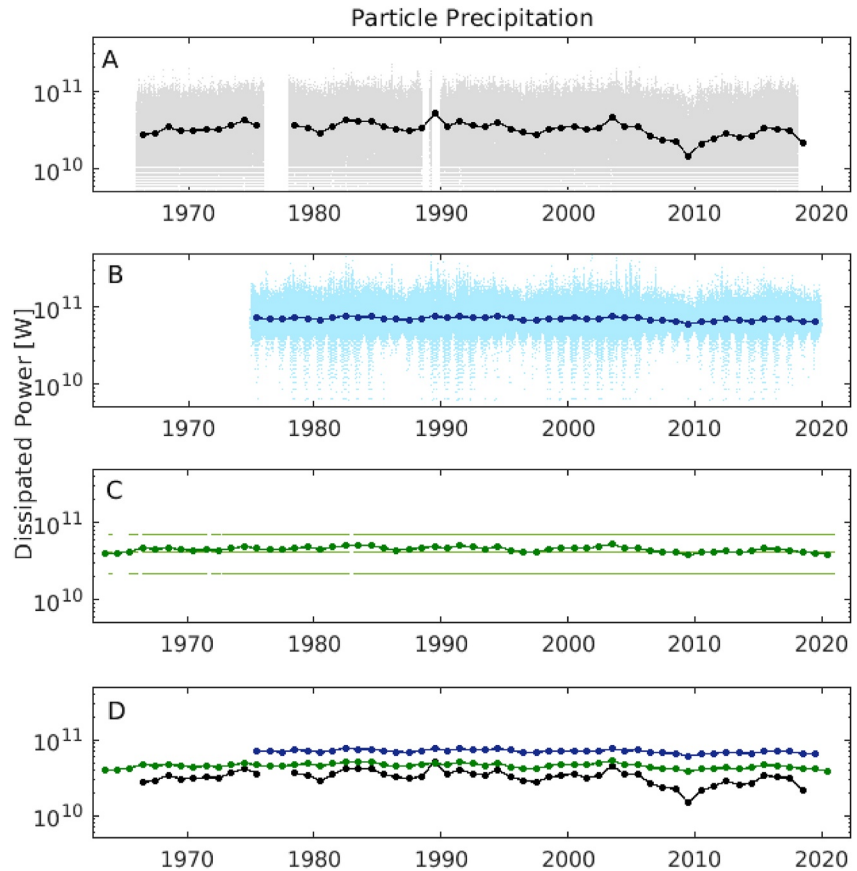
Figure 3. Energy dissipation in the Earth's ionosphere via particle precipitation. Panel (a) estimate from the empirical formula from Tenfjord and Østgaard (2013). Panel (b) estimate from the empirical formula from Chun et al. (2002). Panel (c) estimate from Table 1 in Newell et al. (2009). The scattered points represent the 1 hr averaged dissipated power while the solid lines correspond to the yearly averages (for the estimate presented in panel (c), the 1 hr averaged data points can only take three different values, for low, moderate and strong solar wind driving). Panel D compares the yearly average of the power dissipated via particle precipitation from the three methods using the same colors as in panels (a, b, and c) The yearly averaged dissipated power in 1989 may not be accurate as the AL index is only available for the month of March.

either dissipated in the upper atmosphere or transferred to upflowing electrons in undefined proportions (Keiling et al., 2019). Consequently, we estimate that the Alfven wave energy dissipation in the upper atmosphere corresponds to 11% of the incoming Alfven wave energy as given by Equation 8. The average power dissipated by Alfvén waves in the upper atmosphere during this period is 0.26 GW, much lower than the power dissipated by Joule heating and particle precipitation.

2.4. Result

The solar wind energy flux density is obtained summing the contribution of the solar wind ion kinetic energy and of the Poynting flux. To estimate the total energy flux intercepted by the induced magnetosphere of a hypothetic unmagnetized Earth, we multiply it by the cross section of the induced magnetosphere which is estimated as being a disk with a radius corresponding to the geocentric distance of the IMB at the terminator. It is estimated to 88.2 GW for a radius of the induced magnetosphere of 1.2 R_E, 103.5 GW for a radius of 1.3 R_E and 120 GW for a radius of 1.4 R_E. This corresponds to the maximum solar wind power that could be dissipated in the upper atmosphere of an unmagnetized Earth if all the incoming solar wind power were dissipated in the ionosphere.

This is to be compared with the power dissipated in the atmosphere of the actual (magnetized) Earth. Joule heating and particle precipitation are the two dominant solar wind energy dissipation mechanisms in the Earth's upper atmosphere. Table 1 shows the average value of the total power dissipated in the ionosphere as estimated from the functional forms discussed above. It includes the contribution of Joule heating, particle precipitation and Alfvén

Table 1
Average Power Dissipated in the Upper Atmosphere of the Earth Between 1963 and 2020

			Joule heating (GW)		
			Østgaard, Germany, et al. (2002)	Chun et al. (1999)	Knipp et al. (2005)
			110	110	99.2
			Total dissipated power (GW)[a]		
Particle precipitation (GW)	Tenfjord and Østgaard (2013)	32.4	143	142	132
	Chun et al. (2002)	70.6	181	181	170
	Newell et al. (2009)	45	155	155	144

Note. This table shows the various estimates of the total power dissipated in the upper atmosphere for the various estimates of the dissipated power due to Joule heating and particle precipitation discussed in the text.

[a]It also includes the power dissipated by Alfvén waves (0.26 GW) as estimated from the Keiling et al. (2019) functional forms.

waves. Our estimates of the average dissipated power in the ionosphere from 1963 to 2020 range between 132 and 181 GW with a contribution of Joule heating estimated between 99.2 and 110 GW and a contribution of particle precipitation estimated between 32.4 and 70.6 GW.

3. Discussion

The solar wind energy dissipated in the Earth's upper atmosphere is higher than the solar wind power that would be intercepted by the induced magnetosphere of a hypothetical unmagnetized Earth. This result is valid for all the different methods we used to estimate the energy dissipated in the Earth's upper atmosphere and when considering a larger induced magnetosphere.

It implies, without any assumption on the solar wind energy dissipation in the upper atmosphere of a hypothetical unmagnetized Earth, that the Earth's magnetic field increases solar wind energy dissipation in the upper atmosphere. In order to quantify the increase of energy dissipation due to the magnetization of the Earth, it is necessary to estimate the amount of incoming solar wind energy that would be dissipated in the Earth's upper atmosphere if it were unmagnetized. For the large scale Earth's magnetosphere, the ratio between the solar wind energy transferred into the magnetosphere and the solar wind energy intercepted by the magnetosphere is estimated typically between less than 1% and 10%, the higher values being associated with periods of strong geomagnetic activity when the energy dissipation inside the magnetosphere is high (Knipp et al., 1998; Li et al., 2012; Østgaard, Germany, et al., 2002; Tenfjord & Østgaard, 2013). A fraction of the solar wind energy transferred into the magnetosphere, estimated between 20% and 80% (Guo et al., 2012; Knipp et al., 1998; Østgaard, Germany, et al., 2002), is eventually dissipated in the ionosphere. The induced magnetospheres of Venus and Mars are of much smaller scale. Not all the energy in the solar wind that is intercepted by an unmagnetized planet is imparted to its upper atmosphere, however. Contrary to a low-conductive object without an atmosphere, like the Moon, where the bulk of the solar wind is absorbed by the surface, the ionized part of the planetary atmosphere sets up currents that create a magnetic field opposing the IMF. This IMB diverts the solar wind (Kivelson & Bagenal, 2014; Schunk & Nagy, 2009). Observations at Mars (Fränz et al., 2006; Halekas, Brain, et al., 2017; Halekas, Ruhunusiri, et al., 2017) and Venus (Kollmann et al., 2016; Nordström et al., 2013) show the solar wind being slowed down as it crosses the bow shock and flowing around the IMB with an increased density and temperature, along the magnetic field lines that are draped around the IMB. This IMB is very effective at keeping most of the solar wind out of the dense planetary atmosphere (Brain, 2006) and at diverting the solar wind energy. There is no observational estimate of the coupling efficiency between the solar wind and an induced magnetosphere. However, the average ion escape coupling efficiency (the ratio between the incoming solar wind energy and the energy carried by escaping ions) has been empirically estimated to 0.67 ± 0.04% for Mars (Ramstad, Barabash, Futaana, Nilsson, & Holmström, 2017) and to 0.008% for Venus (Persson et al., 2021). The ion escape efficiency only consider the solar wind energy transferred to escaping ion and not all the solar wind energy that is dissipated in the upper atmosphere. It thus represents a lower limit for the coupling efficiency between the solar wind and the upper atmospheres of Mars and Venus.

The observations discussed above indicate that large scale and induced magnetospheres are efficient at diverting the solar wind and preventing solar wind energy to be dissipated in the upper atmosphere. Thus, the energy that would be dissipated in the upper atmosphere of an unmagnetized Earth would only correspond to a fraction of the incoming solar wind energy. For a coupling efficiency between the solar wind and the upper atmosphere of a hypothetical unmagnetized Earth of 1%, the solar wind energy dissipated in the upper atmosphere would be of the order of ~1 GW meaning that the presence of a large scale magnetic field at Earth would increase the solar wind energy dissipation in its upper atmosphere by a factor of at least 100. For a coupling efficiency of 0.1%, it would be increased by a factor of ~1,000 and by a factor of ~10 for a coupling efficiency of 10%.

Our results thus show with a very high degree of confidence that the presence of a large scale magnetic field substantially increases the solar wind energy deposition in the upper atmosphere of the Earth. The reason behind this increase lies in the interaction between the solar wind and the magnetic environment of planets. Both induced and large scale magnetospheres interact with the solar wind and efficiently shield planetary atmospheres from the solar wind. However, the magnetospheres of magnetized planets like Earth are much larger than the planets themselves. They thus dramatically increase the size of interaction region between the solar wind and the planetary environment and thus the amount of solar wind energy that can potentially be diverted toward the upper atmosphere.

4. Conclusions

It has been shown that the solar wind power currently dissipated in the Earth's upper atmosphere is higher than the solar wind power intercepted by the induced magnetosphere of a hypothetical unmagnetized Earth. This demonstrates a counter-intuitive result: the large scale magnetic field of the Earth increases the solar wind power dissipated in the Earth's upper atmosphere. This conclusion remains valid even if considering the unrealistic situation where all the solar wind energy intercepted by the induced magnetosphere of a hypothetical unmagnetized Earth would end up dissipated in its upper atmosphere. Actually, while of much smaller scale, the induced magnetospheres of unmagnetized planets like Venus and Mars efficiently shields their upper atmosphere from the solar wind. Only a fraction of the solar wind energy intercepted by their induced magnetosphere ends up dissipated in their upper atmosphere. It implies that the increase of solar wind energy dissipation in the upper atmosphere due to the presence of a large scale magnetic field at Earth is significant and can realistically reach a factor of 10 or more. The consequences of this increased energy deposition on atmospheric escape remain to be quantified. However it clearly favors atmospheric escape as more energy is available to accelerate atmospheric material to sufficient energies allowing it to leave the planetary system. Having established that more energy is dissipated in the Earth's upper atmosphere due to the presence of a global magnetic field calls for a re-evaluation of the paradigm that an intrinsic planetary magnetic field minimizes the escape of planetary atmospheres. The results presented in this study are thus relevant not only for understanding the evolution of the Earth's atmosphere but also for understanding the longevity of planetary atmospheres and assessing the habitability of exoplanets.

Data Availability Statement

The data used in this study (in-situ solar wind measurements and geomagnetic activity indices) are publicly available on the GSFC/SPDF OMNIWeb database and can be obtained from its web interface at https://omniweb.gsfc.nasa.gov. We also use empirical formulas derived from observations available in Østgaard, Germany, et al. (2002), Chun et al. (1999), Knipp et al. (2005), Tenfjord and Østgaard (2013), Chun et al. (2002), and Keiling et al. (2019).

References

Brain, D. A. (2006). Mars global surveyor measurements of the Martian solar wind interaction. *Space Science Reviews*, *126*(1–4), 77–112. https://doi.org/10.1007/s11214-006-9122-x

Chun, F. K., Knipp, D. J., McHarg, M. G., Lacey, J. R., Lu, G., & Emery, B. A. (2002). Joule heating patterns as a function of polar cap index. *Journal of Geophysical Research*, *107*(A7), 1119. https://doi.org/10.1029/2001JA000246

Chun, F. K., Knipp, D. J., McHarg, M. G., Lu, G., Emery, B. A., Vennerstrøm, S., & Troshichev, O. A. (1999). Polar cap index as a proxy for hemispheric Joule heating. *Geophysical Research Letters*, *26*(8), 1101–1104. https://doi.org/10.1029/1999GL900196

Fränz, M., Dubinin, E., Roussos, E., Woch, J., Winningham, J. D., Frahm, R., et al. (2006). Plasma moments in the environment of Mars. Mars express ASPERA-3 observations. *Space Science Reviews*, *126*(1–4), 165–207. https://doi.org/10.1007/s11214-006-9115-9

Gronoff, G., Arras, P., Baraka, S., Bell, J. M., Cessateur, G., Cohen, O., et al. (2020). Atmospheric escape processes and planetary atmospheric evolution. *Journal of Geophysical Research: Space Physics*, *125*(8), e2019JA027639. https://doi.org/10.1029/2019JA027639

Gunell, H., Maggiolo, R., Nilsson, H., Stenberg Wieser, G., Slapak, R., Lindkvist, J., et al. (2018). Why an intrinsic magnetic field does not protect a planet against atmospheric escape. *Astronomy & Astrophysics*, *614*, L3. https://doi.org/10.1051/0004-6361/201832934

Guo, J., Feng, X., Emery, B. A., & Wang, Y. (2012). Efficiency of solar wind energy coupling to the ionosphere. *Journal of Geophysical Research*, *117*(A7), A07303. https://doi.org/10.1029/2012JA017627

Halekas, J. S., Brain, D. A., Luhmann, J. G., DiBraccio, G. A., Ruhunusiri, S., Harada, Y., et al. (2017). Flows, fields, and forces in the Mars-solar wind interaction. *Journal of Geophysical Research: Space Physics*, *122*(11), 11320–11341. https://doi.org/10.1002/2017JA024772

Halekas, J. S., Ruhunusiri, S., Harada, Y., Collinson, G., Mitchell, D. L., Mazelle, C., et al. (2017). Structure, dynamics, and seasonal variability of the Mars-solar wind interaction: MAVEN solar wind ion analyzer in-flight performance and science results. *Journal of Geophysical Research: Space Physics*, *122*(1), 547–578. https://doi.org/10.1002/2016JA023167

Hartinger, M. D., Moldwin, M. B., Zou, S., Bonnell, J. W., & Angelopoulos, V. (2015). ULF wave electromagnetic energy flux into the ionosphere: Joule heating implications. *Journal of Geophysical Research: Space Physics*, *120*(1), 494–510. https://doi.org/10.1002/2014JA020129

Keiling, A., Thaller, S., Wygant, J., & Dombeck, J. (2019). Global Alfvén wave power in the auroral zone in relation to the AE index. *Journal of Geophysical Research: Space Physics*, *124*(11), 8637–8646. https://doi.org/10.1029/2019JA026805

Kivelson, M. G., & Bagenal, F. (2014). Planetary magnetospheres. In *Encyclopedia of the solar system* (pp. 137–157). Elsevier.

Knipp, D. J., Emery, B. A., Engebretson, M., Li, X., McAllister, A. H., Mukai, T., et al. (1998). An overview of the early November 1993 geomagnetic storm. *Journal of Geophysical Research*, *103*(A11), 26197–26220. https://doi.org/10.1029/98JA00762

Knipp, D. J., Welliver, T., McHarg, M. G., Chun, F. K., Tobiska, W. K., & Evans, D. (2005). Climatology of extreme upper atmospheric heating events. *Advances in Space Research*, *36*(12), 2506–2510. https://doi.org/10.1016/j.asr.2004.02.019

Kollmann, P., Brandt, P. C., Collinson, G., Rong, Z. J., Futaana, Y., & Zhang, T. L. (2016). Properties of planetward ion flows in Venus' magnetotail. *Icarus*, *274*, 73–82. https://doi.org/10.1016/j.icarus.2016.02.053

Le Chat, G., Issautier, K., & Meyer-Vernet, N. (2012). The solar wind energy flux. *Solar Physics*, *279*(1), 197–205. https://doi.org/10.1007/s11207-012-9967-y

Li, H., Wang, C., Xu, W. Y., & Kan, J. R. (2012). Characteristics of magnetospheric energetics during geomagnetic storms. *Journal of Geophysical Research*, *117*(A4), A04225. https://doi.org/10.1029/2012JA017584

Lockwood, M. (2019). Does adding solar wind Poynting flux improve the optimum solar wind-magnetosphere coupling function? *Journal of Geophysical Research: Space Physics*, *124*(7), 5498–5515. https://doi.org/10.1029/2019JA026639

Maggiolo, R., & Gunell, H. (2021). Does a magnetosphere protect the ionosphere? In *Magnetospheres in the solar system* (pp. 729–742). American Geophysical Union (AGU). https://doi.org/10.1002/9781119815624.ch45

Maggiolo, R., Hamrin, M., De Keyser, J., Pitkänen, T., Cessateur, G., Gunell, H., & Maes, L. (2017). The delayed time response of geomagnetic activity to the solar wind. *Journal of Geophysical Research: Space Physics*, *122*(11), 11109–11127. https://doi.org/10.1002/2016JA023793

Matsunaga, K., Seki, K., Brain, D. A., Hara, T., Masunaga, K., Mcfadden, J. P., et al. (2017). Statistical study of relations between the induced magnetosphere, ion composition, and pressure balance boundaries around Mars based on MAVEN observations. *Journal of Geophysical Research: Space Physics*, *122*(9), 9723–9737. https://doi.org/10.1002/2017JA024217

Newell, P. T., Sotirelis, T., Liou, K., Meng, C.-I., & Rich, F. J. (2007). A nearly universal solar wind-magnetosphere coupling function inferred from 10 magnetospheric state variables. *Journal of Geophysical Research*, *112*(A1), A01206. https://doi.org/10.1029/2006JA012015

Newell, P. T., Sotirelis, T., & Wing, S. (2009). Diffuse, monoenergetic, and broadband aurora: The global precipitation budget. *Journal of Geophysical Research*, *114*(A9), A09207. https://doi.org/10.1029/2009JA014326

Nordström, T., Stenberg, G., Nilsson, H., Barabash, S., & Zhang, T. L. (2013). Venus ion outflow estimates at solar minimum: Influence of reference frames and disturbed solar wind conditions. *Journal of Geophysical Research: Space Physics*, *118*(6), 3592–3601. https://doi.org/10.1002/jgra.50305

Østgaard, N., Germany, G., Stadsnes, J., & Vondrak, R. R. (2002). Energy analysis of substorms based on remote sensing techniques, solar wind measurements, and geomagnetic indices. *Journal of Geophysical Research*, *107*(A9), SMP9-1–SMP9-14. https://doi.org/10.1029/2001JA002002

Østgaard, N., Vondrak, R. R., Gjerloev, J. W., & Germany, G. (2002). A relation between the energy deposition by electron precipitation and geomagnetic indices during substorms. *Journal of Geophysical Research*, *107*(A9), 1246. https://doi.org/10.1029/2001JA002003

Persson, M., Futaana, Y., Ramstad, R., Schillings, A., Masunaga, K., Nilsson, H., et al. (2021). Global venus-solar wind coupling and oxygen ion escape. *Geophysical Research Letters*, *48*(3), e2020GL091213. https://doi.org/10.1029/2020GL091213

Rae, I. J., Watt, C. E. J., Fenrich, F. R., Mann, I. R., Ozeke, L. G., & Kale, A. (2007). Energy deposition in the ionosphere through a global field line resonance. *Annales Geophysicae*, *25*(12), 2529–2539. https://doi.org/10.5194/angeo-25-2529-2007

Ramstad, R., & Barabash, S. (2021). Do intrinsic magnetic fields protect planetary atmospheres from stellar winds? *Space Science Reviews*, *217*(2), 36. https://doi.org/10.1007/s11214-021-00791-1

Ramstad, R., Barabash, S., Futaana, Y., & Holmström, M. (2017). Solar wind- and EUV-dependent models for the shapes of the Martian plasma boundaries based on Mars Express measurements. *Journal of Geophysical Research: Space Physics*, *122*(7), 7279–7290. https://doi.org/10.1002/2017JA024098

Ramstad, R., Barabash, S., Futaana, Y., Nilsson, H., & Holmström, M. (2017). Global Mars-solar wind coupling and ion escape. *Journal of Geophysical Research: Space Physics*, *122*(8), 8051–8062. https://doi.org/10.1002/2017JA024306

Schunk, R., & Nagy, A. (2009). *Ionospheres: Physics, plasma physics, and chemistry* (2nd ed.). Cambridge University Press. https://doi.org/10.1017/CBO9780511635342

Schwenn, R. (1990). Large-scale structure of the interplanetary medium. In R. Schwenn & E. Marsch (Eds.), *Physics of the inner heliosphere i* (p. 99).

Tenfjord, P., & Østgaard, N. (2013). Energy transfer and flow in the solar wind-magnetosphere-ionosphere system: A new coupling function. *Journal of Geophysical Research: Space Physics*, *118*(9), 5659–5672. https://doi.org/10.1002/jgra.50545

Thorne, R. M., Bortnik, J., Li, W., & Ma, Q. (2021). Wave–particle interactions in the Earth's magnetosphere. In *Magnetospheres in the solar system* (pp. 93–108). American Geophysical Union (AGU). https://doi.org/10.1002/9781119815624.ch6

Trotignon, J., Mazelle, C., Bertucci, C., & Acuña, M. (2006). Martian shock and magnetic pile-up boundary positions and shapes determined from the Phobos 2 and Mars Global Surveyor data sets. *Planetary and Space Science*, *54*(4), 357–369. https://doi.org/10.1016/j.pss.2006.01.003

Vasyliūnas, V. M., & Song, P. (2005). Meaning of ionospheric Joule heating. *Journal of Geophysical Research*, *110*(A2), A02301. https://doi.org/10.1029/2004JA010615

Wing, S., Johnson, J. R., Chaston, C. C., Echim, M., Escoubet, C. P., Lavraud, B., et al. (2014). Review of Solar wind entry into and transport within the plasma sheet. *Space Science Reviews*, *184*(1–4), 33–86. https://doi.org/10.1007/s11214-014-0108-9

Zhang, T. L., Delva, M., Baumjohann, W., Volwerk, M., Russell, C. T., Wei, H. Y., et al. (2008). Induced magnetosphere and its outer boundary at Venus. *Journal of Geophysical Research*, *113*(E9), E00B20. https://doi.org/10.1029/2008JE003215